

**Electronic Supplementary Information:**

**The role of crystallinity of palladium nanocrystals in ROS generation  
and cytotoxicity induction**

Yanxin Wu<sup>1,#</sup>, Rongtao Liu<sup>1,#</sup>, Jian Liu<sup>1</sup>, Jianbo Jia<sup>1</sup>, Hongyu Zhou<sup>1\*</sup>, Bing Yan<sup>1</sup>

<sup>1</sup>Institute of Environmental Research at Greater Bay, Key Laboratory for Water Quality and Conservation of the Pearl River Delta, Ministry of Education, Guangzhou University, Guangzhou, Guangdong, 510006, China

<sup>#</sup>These authors contributed equally to this work.

**\*Corresponding author**

Hongyu Zhou (hyzhou001@gzhu.edu.cn)

The concentrations of Pd nanocrystals were calculated to maintain the equivalent for surface atoms of samples, according to *SI Eq(1-1)~ (1-6)*.

$$\text{PdNCs} \quad N = 12m^2 - 24m + 14 \quad \text{Eq(1-1)}$$

$$\text{PdNOs} \quad N = 4m^2 - 8m + 6 \quad \text{Eq(1-2)}$$

$$\text{PdNTs} \quad N = 2m^2 - 4m + 4 \quad \text{Eq(1-3)}$$

$$\text{PdNCTs} \quad N_{\{111\}} = \frac{3}{2}m^2 - 2m \quad \text{Eq(2-4)}$$

$$N_{\{110\}} = \frac{1}{36}m^2 - \frac{2}{3}m + 8 \quad \text{Eq(2-5)}$$

$$N_{\text{Total}} = \frac{55}{36}m^2 - \frac{8}{3}m + 8 \quad \text{Eq(2-6)}$$

Calculations were performed by assuming that all the nanocrystals had perfect morphologies.  $m$ , defined as the number of atoms lying on an equivalent edge (corner atoms included).  $N$ , defined as the number of surface atoms.

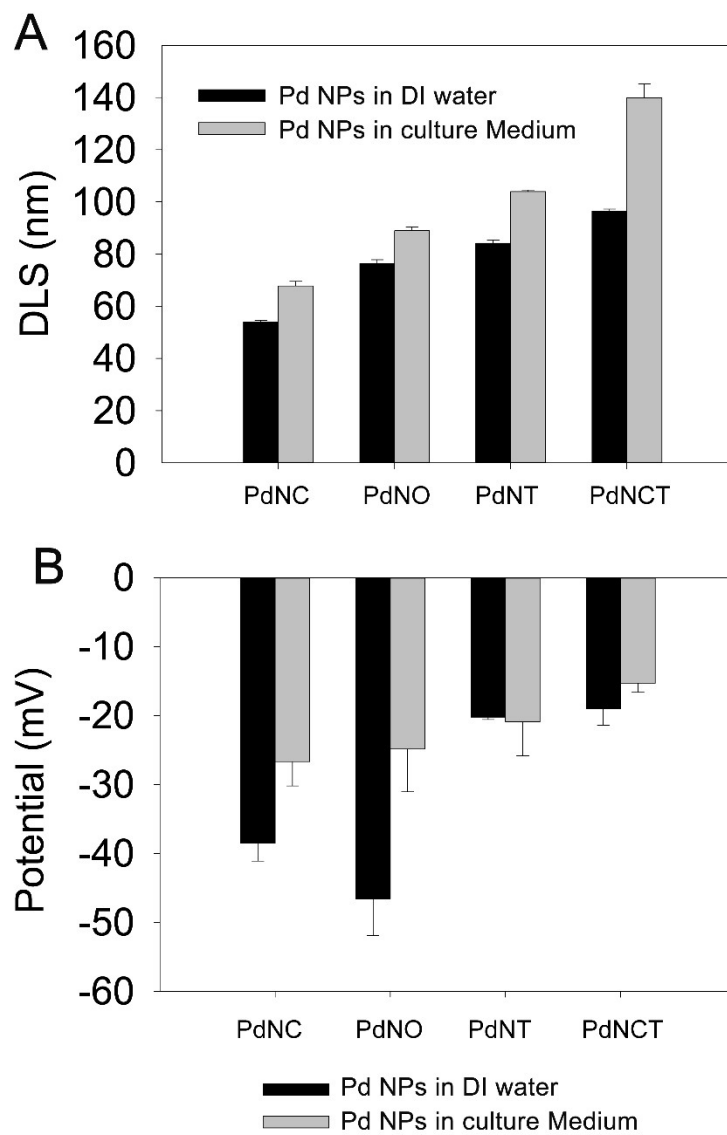


**Fig. S1** DLS and zeta potential measurement of different Pd nanocrystals in deionized water or cell culture medium with 10% fetal bovine serum.

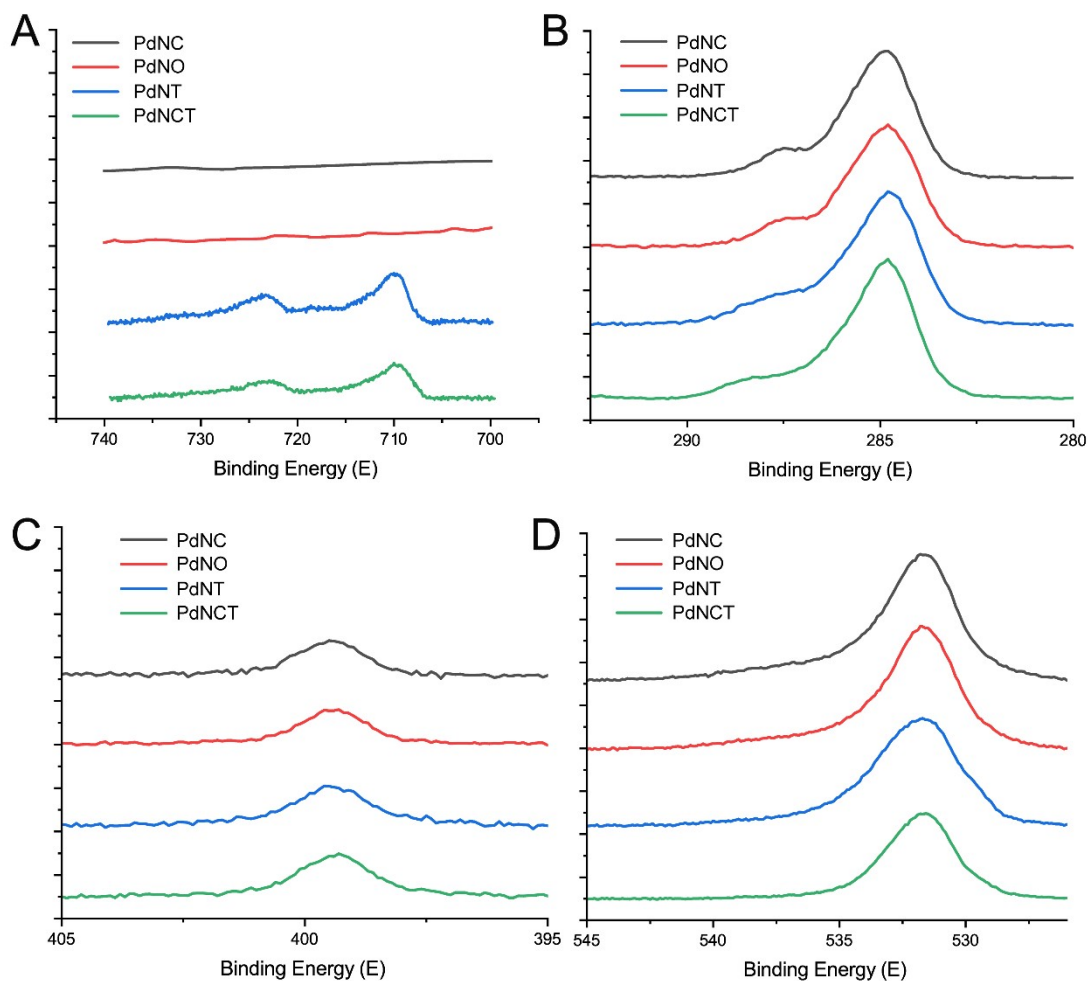


**Fig. S2** XPS characterizations of different Pd crystals. (A) Fe2p, (B) C1s, (C) N1s, and (D) O1s high resolution XPS spectra.

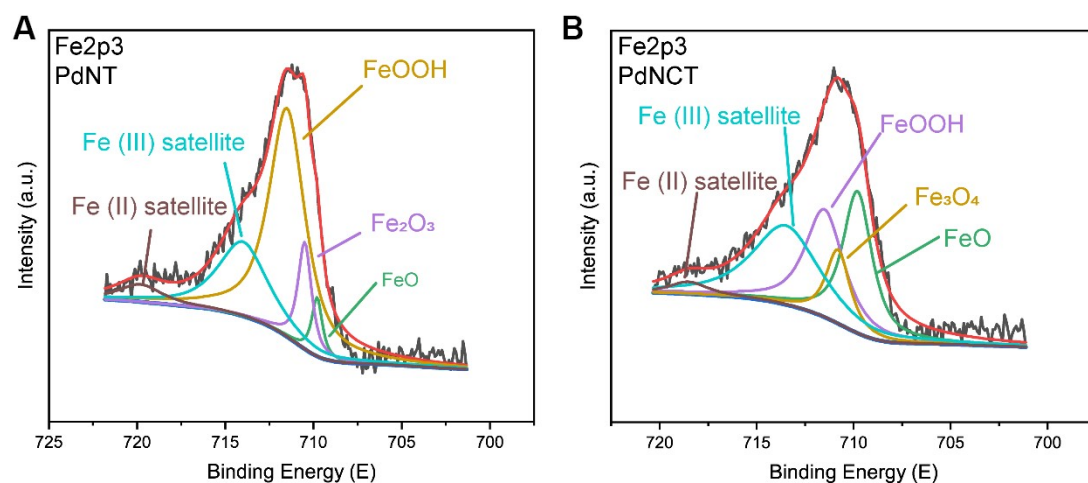


**Fig. S3** High-resolution XPS Fe2p3 spectra of (A) PdNT and (B) PdNCT.

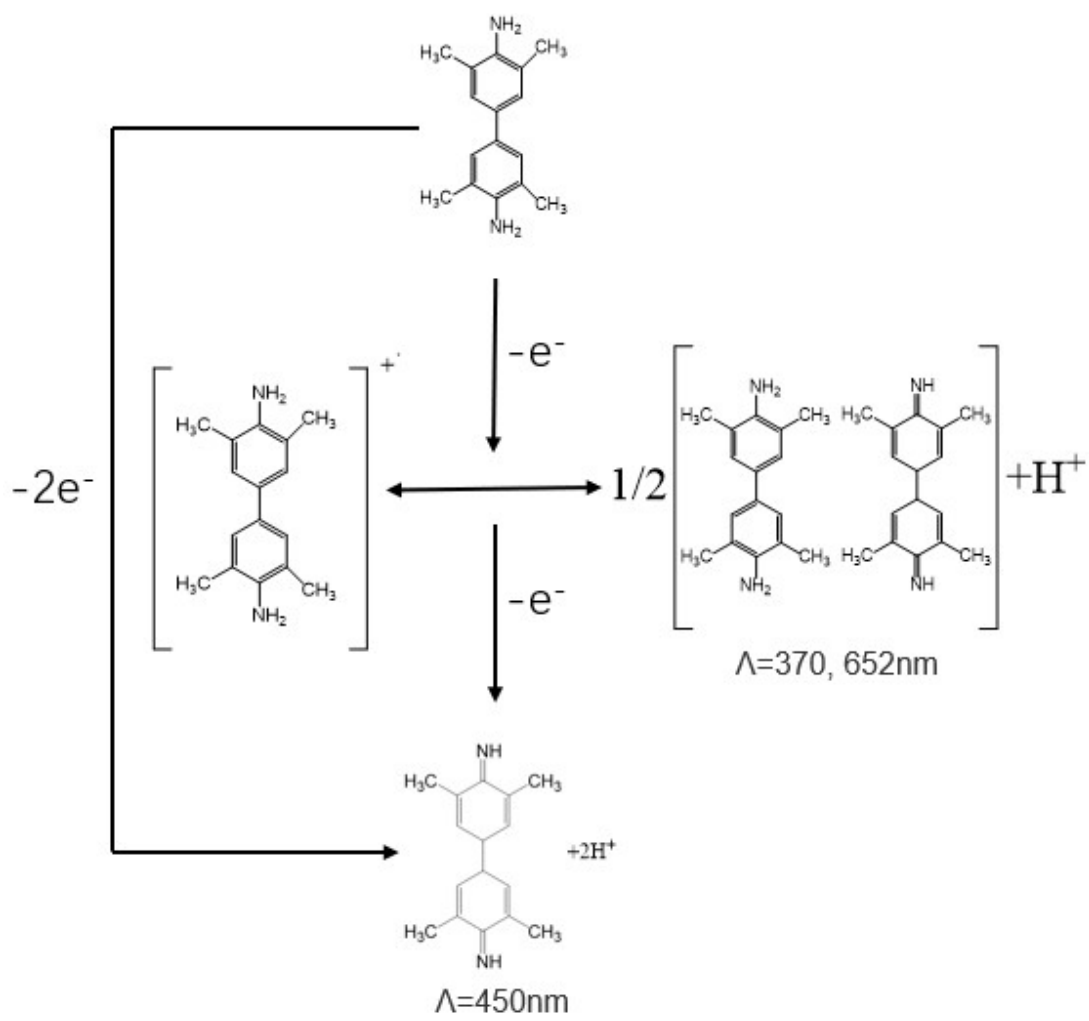


**Fig. S4** Luminescence mechanism of TMB probe

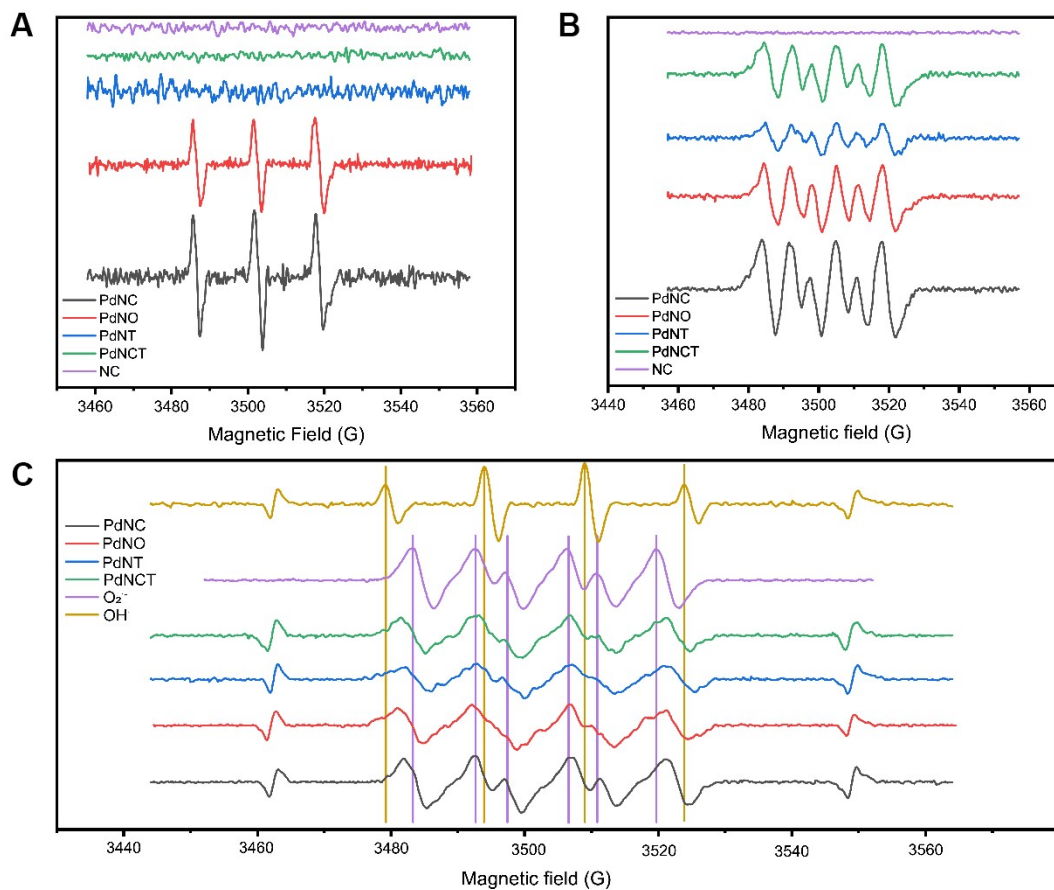


**Fig. S5** ESR measurements. (A) ESR spectra of the samples after mixing 4-oxo-TMP solution with Pd nanocrystals to detect  $^1\text{O}_2$  (B) ESR spectra of samples containing BMPO, DPTA, and Pd nanocrystals. (C) ESR spectra of samples including DMPO, Pd nanocrystals –  $\text{H}_2\text{O}_2$  system with the  $\text{Mn}^{2+}$  marker.

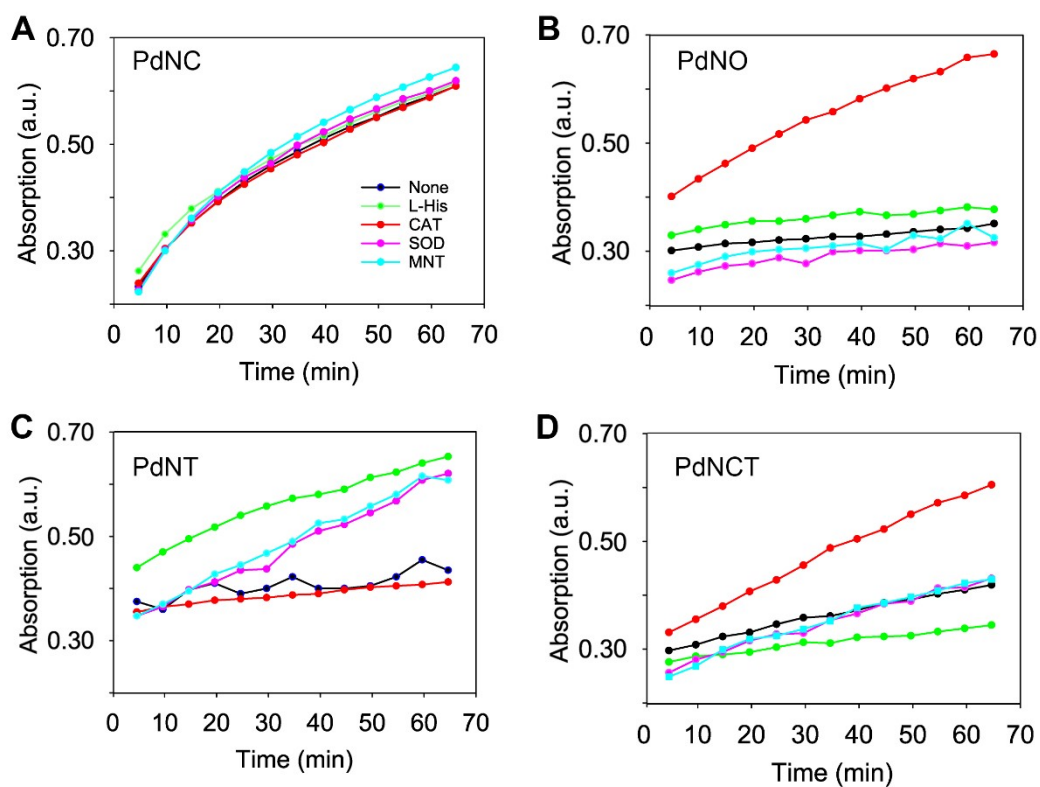


**Fig. S6** The single-electron oxidation product at 652nm when TMB mixed with different crystals and ROS scavengers. (A) PdNCs, (B) PdNOs, (C) PdNTs, (D) PdNCTs.

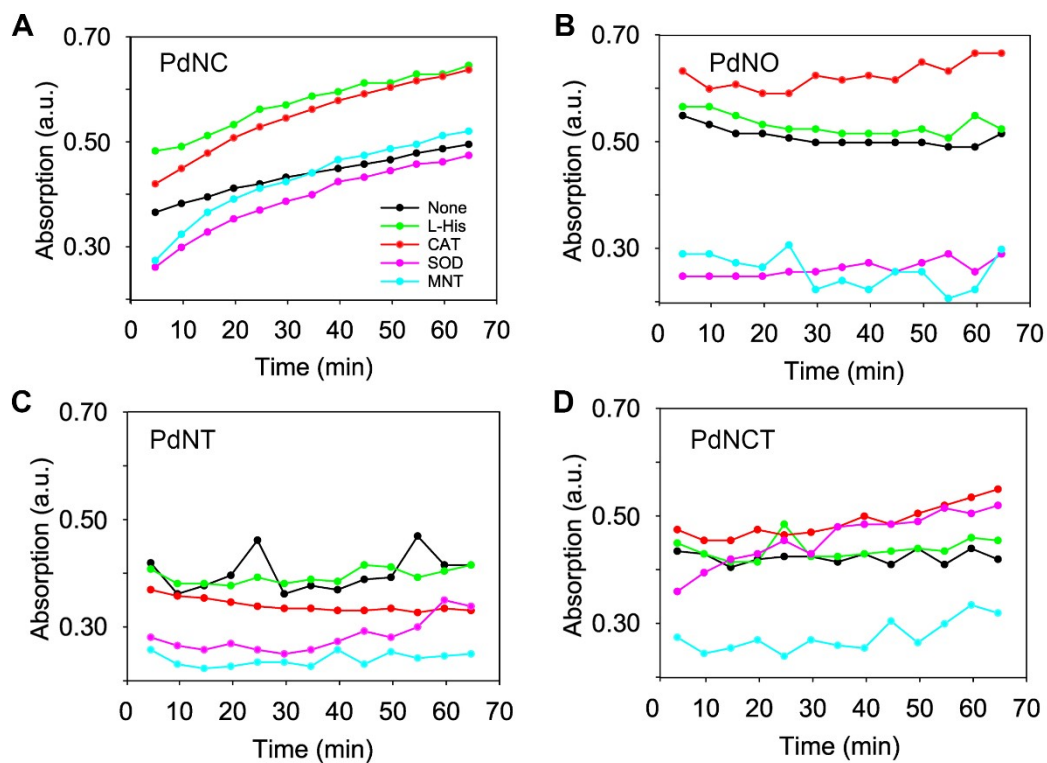


**Fig. S7** The completed oxidation product at 450nm when TMB mixed with Pd nanocrystals and different ROS scavengers. (A) PdNCs, (B) PdNOs, (C) PdNTs, (D) PdNCTs.



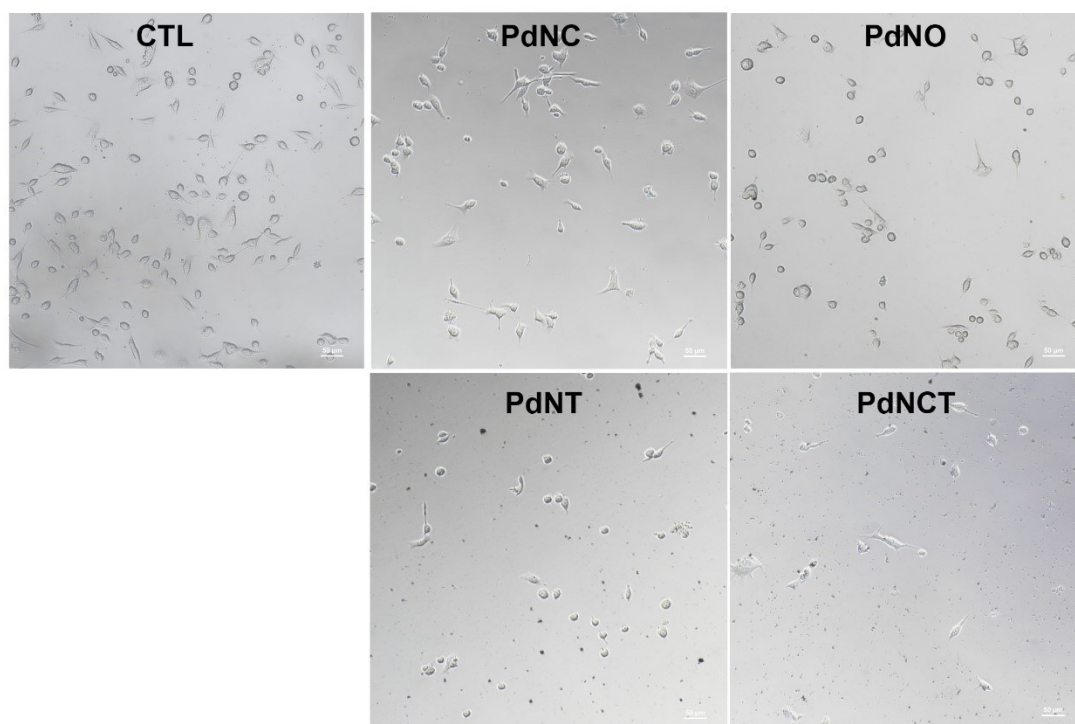


**Fig. S8** Representative photographs of GES-1 cells treated with culture medium (CTL) or different Pd nanocrystals at 7  $\mu\text{g}/\text{mL}$  for 24 h.

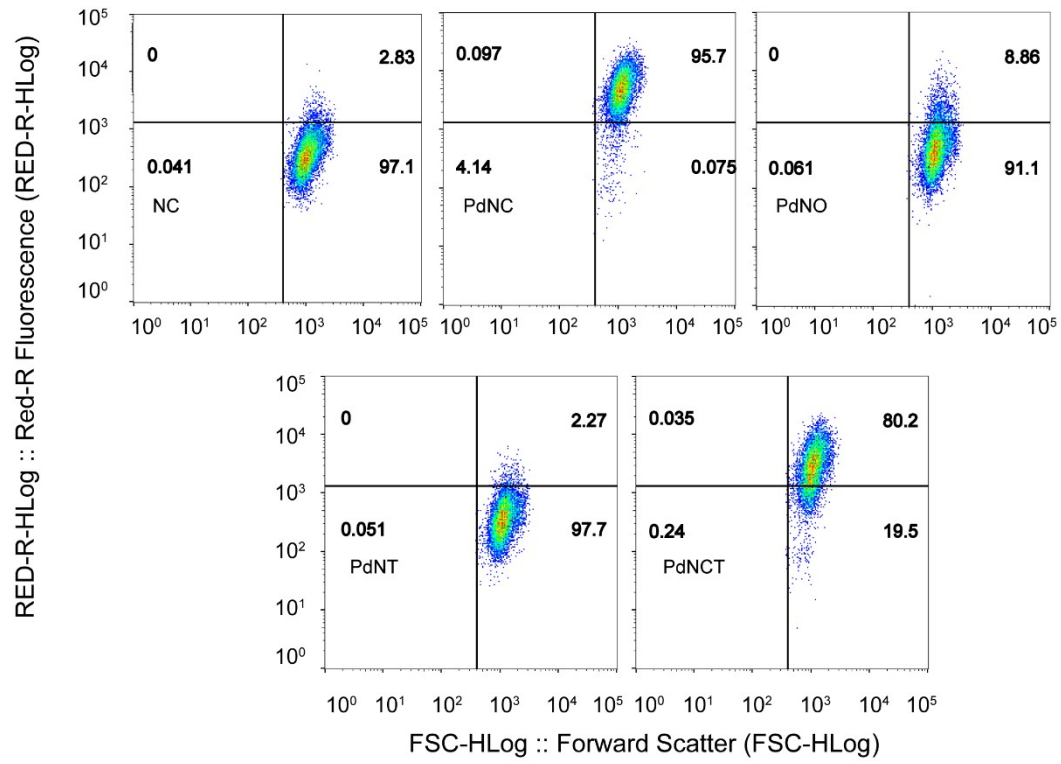


**Fig. S9** HO-1 expression measurement through flow cytometry analysis. NC: Negative Control.

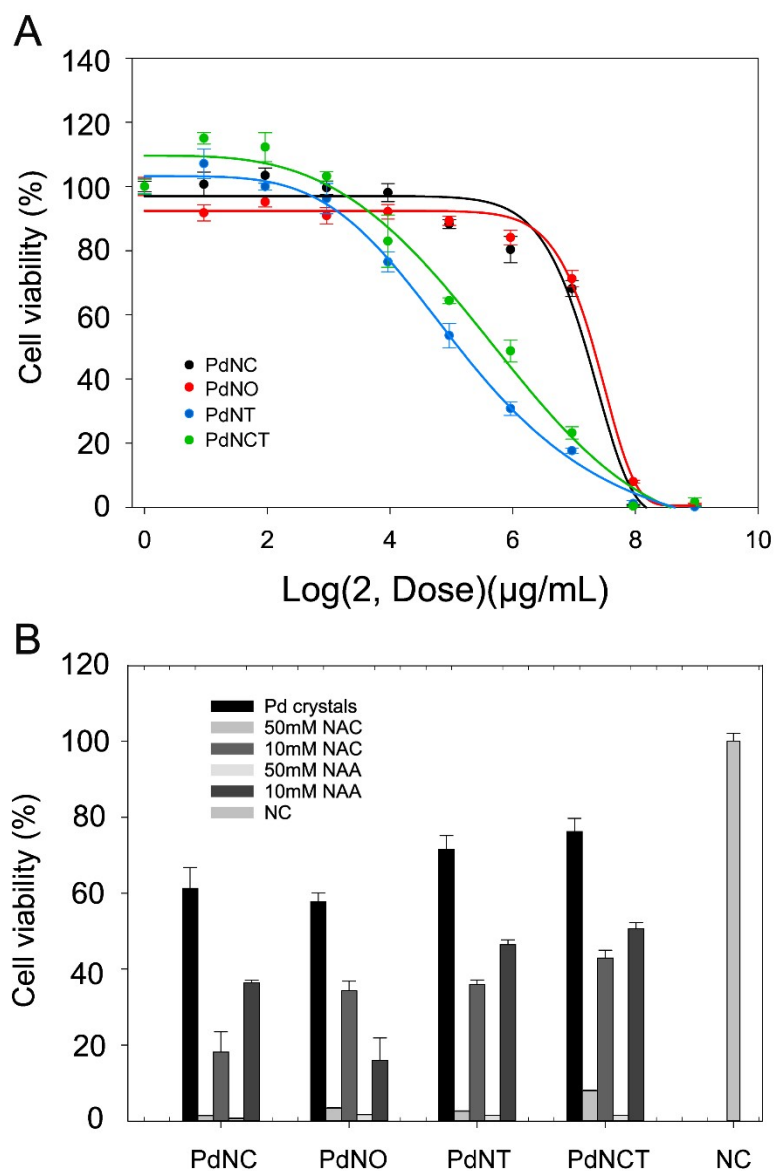


**Fig. S10** Cell viability experiments of Pd crystals in MCF-7 cell lines. (A) Dose-response curves. (B) Pd crystals incubated with 50/10 mM NAC/NAA.